

Aging processes and scale dependence in soft glassy colloidal suspensionsM. Bellour,¹ A. Knaebel,¹ J. L. Harden,² F. Lequeux,³ and J.-P. Munch^{1,*}¹*LDFC, CNRS UMR 7506, 3 rue de l'Université, 67084 Strasbourg, France*²*Department of Chemical Engineering, Johns Hopkins University, Baltimore, Maryland 21218-2689*³*LPM, CNRS UMR 7615, ESPCI, 10 rue Vauquelin, 75005 Paris, France*

(Received 29 July 2002; published 25 March 2003)

The aging behavior of colloidal suspensions of laponite, a model synthetic clay, is investigated using light scattering techniques. In order to measure the complete dynamic structure factor as a function of time and of wave vector, we have developed an original optical setup using a multispeckle technique for simple light scattering. We have thus measured the correlation of the scattered light intensity as a function of the age of the sample t_w for various concentrations. For sufficiently concentrated samples, we observe a two-stage relaxation process. The fast relaxation is diffusive, stationary, and reminiscent of the liquidlike behavior observed in less concentrated samples. The slow relaxation behavior, however, is more complex. It exhibits two successive regimes as the sample ages. In the first regime, the decay time τ_a increases exponentially with t_w as long as $\tau_a < t_w$. In the second one, “full aging” is observed in which τ_a is proportional to t_w . In this second regime, the relaxation of concentration fluctuations are hyperdiffusive, scaling as $\exp[-(t/\tau_a)^\beta]$ with $\beta = 1.35 \pm 0.15$. In addition, the spatial dependence of this relaxation time scales as $\tau_a(q) \sim q^{-x}$ with $x \approx 1.3$.

DOI: 10.1103/PhysRevE.67.031405

PACS number(s): 82.70.Dd, 64.70.Pf, 61.20.Lc, 83.85.Ei

I. INTRODUCTION

Suspensions of charged anisotropic colloidal particles such as clay are ubiquitous in nature and are of broad technological importance [1–3]. Under conditions of low ionic strength and suitable pH , repulsive interactions between charged colloidal particles can lead to liquidlike suspensions for low particle concentrations. With increasing volume fraction, interparticle repulsion leads to restricted mobility of the colloidal particles. Eventually, such suspensions often become jammed in a glassy state. Typically, this jamming transition occurs at a characteristic volume fraction ϕ^* at which the counterion clouds of neighboring particles overlap.

For suspensions of repulsive spherical colloidal particles, this transition occurs at relatively high volume fractions ($\phi^* \gtrsim 0.50$). However, highly anisotropic particles, such as clays, can form glassy phases at very low particle volume fractions ($\phi^* \approx 0.01$). These glassy phases are rather diffuse, and as a result have unusual dynamical properties. On macroscopic length scales, such glassy colloidal suspensions have mechanical properties characteristic of metastable soft solids, including solidlike behavior with a finite yield stress, thixotropic response to applied deformation, and slow recovery after deformation [4–6]. Moreover, the mechanical properties of such suspensions may continuously evolve with time [6,7]. This so-called “aging” phenomena is indicative of systems that are far from equilibrium [8,9]. It has been proposed that many of these properties are associated with the metastable, heterogeneous structure of soft materials on microscopic to mesoscopic length scales [10,11]. Recent work has explored the connection between jamming and glassy behavior in soft materials [12]

In this paper, we present dynamic light scattering studies

of aqueous suspensions of laponite, a model synthetic hectorite clay. The physical chemistry and phase behavior of laponite has been well characterized [13–16], allowing us to focus on its dynamical properties. Stable, homogeneous solutions are produced when dry laponite is rehydrated in stirred deionized water, filtered, and stored under conditions of high pH and low ionic strength. Low concentration suspensions ($\phi < \phi^* \approx 0.7\%$) form stable, equilibrium fluid phases. Higher concentration suspensions ($\phi \gtrsim \phi^*$) are initially fluid. However, after the cessation of mixing, which defines a quench into the glassy phase [12], they gradually thicken with time and become soft glassy solids [17–22]. This glassy phase is metastable and has been shown to exhibit fascinating aging behavior [20–22].

Here, we investigate the spatial dependence of the dynamical behavior of laponite suspensions during aging. More precisely, we look at the relaxation of concentration fluctuations through the measurement of the dynamic structure factor $f(q, t, t_w)$. In salt-free laponite solutions, two distinct scaling behaviors for aging have been observed experimentally by different authors: exponential aging [21]—an exponential increase of the slow relaxation time with the age of the system—and “full aging” [22]—a linear increase of the relaxation time with t_w . Our main aim of this paper is to clarify this experimental situation. In a previous publication [22], we have observed full aging using diffusing wave spectroscopy (DWS) on laponite suspensions containing latex particles. Here, we present detailed results using simple light scattering on the aging properties of laponite suspensions without latex particles, showing that both exponential and full aging successively occur in salt-free laponite suspensions during the aging process. The paper is organized as follows. First, we describe the system and the sample preparation protocol. We then present the optical methods that we have used and the experimental setup for this study. Finally, we present and discuss our experimental results.

*Author to whom correspondence should be addressed.

II. EXPERIMENT

A. Sample preparation

Laponite RD (Laporte Ltd.), a synthetic hectorite clay consisting of relatively monodisperse, disc-shaped particles of mean diameter $d \approx 30$ nm and thickness $\ell \approx 1$ nm, was obtained from Southern Clay Products (Gonzales, Texas). These clay particles are composed of a central sheet of octahedrally coordinated magnesium ions (with lithium ion substitution) between two tetrahedrally coordinated silica sheets. Substitution of lithium for magnesium in the central sheet gives rise to a net negative charge on the faces of the particles that is balanced by sodium counterions. The counterions become unbound when laponite is dispersed in aqueous solution, leading to a charged colloidal suspension. The edge charge of a laponite particle is pH dependent [13]. At high pH , the edge charge is negative, implying overall repulsive electrostatic interactions between laponite particles in solution.

A detailed phase diagram for laponite suspensions at high pH as a function of ionic strength and laponite volume fraction has previously been established [15]. At low ionic strength and high pH , increasing laponite volume fraction leads to a transition from a liquidlike phase to a solidlike phase in which the system becomes jammed in a glassy state. This transition occurs at very low volume fraction ($\phi \approx 0.7\%$) due to repulsive interactions and shape anisotropy of particles. At the transition, the disordered liquidlike structure remains essentially unchanged and these jammed systems evolve spontaneously in the absence of external forcing. They are said to age [9,11], meaning that their mechanical and dynamical properties evolve in time [6,7,20–22]. Moreover, the jammed system can be refluidized by applying a stress. For instance, sufficiently strong vortex mixing can liquefy glassy laponite suspensions. After the cessation of such mixing, the suspension is requenched into the glassy state, and the system once again starts aging.

Aqueous suspension of laponite RD for light scattering measurements were prepared at various volume fractions ranging from $\phi = 0.039\%$ ($c \approx 0.1$ wt %) to $\phi = 1.36\%$ ($c \approx 3.5$ wt %) by mixing oven-dried clay in stirred 18 M Ω deionized water for 2 h, and filtering the clarified solutions through 0.45 μm cellulose acetate filters (millipore), in order to breakup particle aggregates that would otherwise lead to spurious small angle scattering [18]. The age t_w of a sample is measured from this filtering time. Samples for static and dynamic light scattering studies were stored in seal vials under nitrogen to prevent sample acidification due to dissolved CO_2 [16]. The resulting solutions have $pH \approx 9.8$ and ionic strength $I \leq 5 \times 10^{-4}$ M. For sufficient low volume fractions, $\phi < \phi^* \approx 0.7\%$ ($c \leq 1.8$ wt %), these phases are stable liquid suspensions. However, for $\phi \geq \phi^*$ these suspensions evolve into homogeneous, charge stabilized glassy phases after a sufficiently induction period [14–22].

B. Methods for dynamic light scattering measurements

We employed several methods for dynamic light scattering (DLS) studies on laponite suspensions. For liquid

samples ($\phi < \phi^*$) that behave like ergodic systems in scattering experiments, we used a standard light scattering setup, in conjunction with a fast multiple-tau digital correlator (ALV 5000). For glassy solid samples that exhibit a two-stage relaxation process, the slow relaxations are evolving with time. This requires that the dynamic structure factor be obtained by performing ensemble-averaged DLS measurements. We used two different methods to do this ensemble averaging. The first one probes the short time behavior ($t < 10^{-2}$ s), while the second one characterizes slower dynamics. The first method is classical and involves slowly rotating the samples in the device, while performing standard time-averaged DLS measurements. Sample rotation introduces an artificial decorrelation time of $\tau_d = 100$ ms in our case.

For slower dynamics, we have developed a “multi-speckle” technique that is similar to previously developed methods [23,24], but not devoted to small angle scattering. Our setup also allows one to perform a real time measurement of the evolution of the correlation function. This multispeckle technique involves using a charge-coupled device (CCD) camera as a detector for scattered intensity. In our setup each pixel of the CCD chip is used as a light detector, allowing for the collection of light scattered by distinct ensembles of scatterers in the sample at the same wave vector q . This approach allows one to compute an ensemble-average correlation function of the scattered light. In practice, we have modified our standard light scattering set up as follows: first the laser beam is expanded into a sheet of light (thickness 0.1 mm and height 15 mm) using a cylindrical plano-concave lens [Fig. 1(a)]. The cell consists in a simple parallelepipedal glass container, and is not immersed in a fluid. There is no thermostat and all the experiments were performed at 20 °C. Then, by adding an afocal system consisting of two lenses and a pinhole (100 μm) between the CCD camera and the sample [Fig. 1(b)], the intensity of scattered light from different portions of this sheet is collected at a fixed scattering angle. The pinhole diameter and focal distance of the lens are chosen in such a way that the size of one speckle is of the same order of magnitude as the size of one pixel ($6 \times 8 \mu\text{m}^2$). Thus, it is possible to monitor simultaneously a large number of speckles (of order 10^5) in parallel. The resulting ensemble-averaged intensity correlation function at a fixed wave number q is given by

$$g^{(2)}(q, t, t_w) = \frac{\langle I_{ij}(q, t_w) I_{ij}(q, t_w + t) \rangle_{ij}}{\langle I_{ij}(q, t_w) \rangle_{ij} \langle I_{ij}(q, t_w + t) \rangle_{ij}}, \quad (1)$$

$\langle \dots \rangle_{ij}$ denotes an ensemble average, where ij defines the pixel-source couple $P_{ij} - S_{ij}$. From this ensemble-averaged intensity correlation function, we define a snapshot dynamic structure factor at t_w ,

$$f(q, t, t_w) = [g^{(2)}(q, t, t_w) - 1]^{1/2}. \quad (2)$$

Figure 2 shows an example of the dynamic structure factor measured by the two techniques described above. The dashed line represents the artificial decorrelation time due to the sample rotation. Linking up of the two distinct parts of

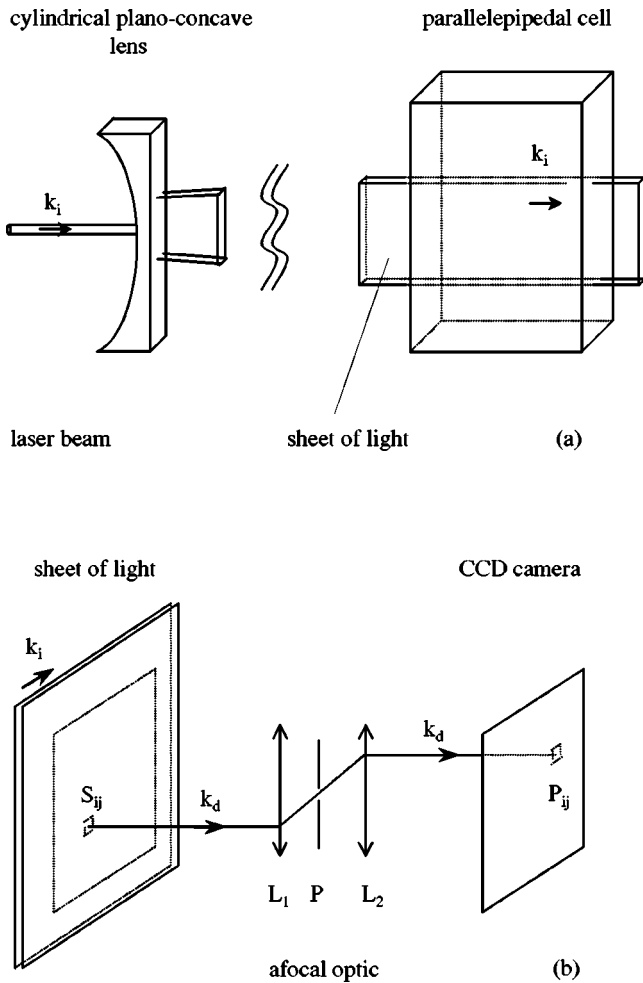


FIG. 1. Experimental setup. (a) The incident laser beam is expanded into a “sheet” of light (thickness 0.1 mm and height 20 mm) using a cylindrical plano-concave lens. (b) The intensity of the scattered light is collected at a fixed scattering angle and imaged onto a CCD chip using an afocal system consisting of two lenses and a pinhole aperture.

the dynamic structure factor is achieved using a reference stationary sample that displays a well known intermediate plateau over a range of t accessible to both techniques or by overlapping common parts of correlation functions measured by the two methods. Finally, let us insist on one point. Aging behavior is very sensitive to mechanical noise. In practice, it was impossible to rotate the arm supporting the CCD and its optics during the experiments without perturbing the system. Thus, we have used two CCD devices at the same time to characterize the same aging behavior of the same sample. However, this noise sensitivity forbids very precise determination of the q dependence of aging. In the following section, we examine the static and dynamic structure factors of the laponite suspensions using this setup.

III. RESULTS

A. Static light scattering experiments

Static light scattering experiments on laponite suspensions with volume fractions between $\phi = 0.039\%$ and $\phi = 1.36\%$

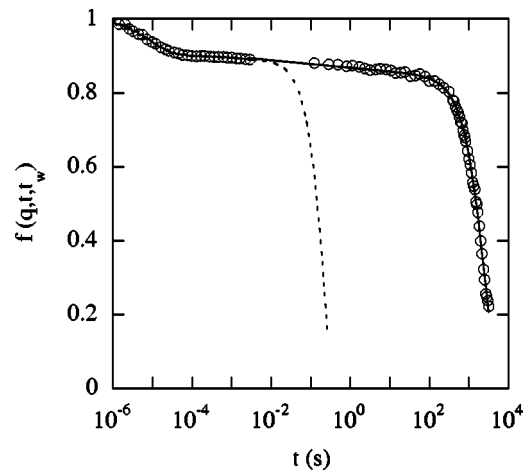


FIG. 2. Complete dynamic structure factor of a glassy laponite suspension ($\phi = 1.36\%$) measured at $q = 0.02422 \text{ nm}^{-1}$ ($\theta = 90^\circ$) by two complementary techniques using a photomultiplier and a CCD chip as light detector. The dashed line represents the decorrelation time due to sample rotation.

were investigated using a standard light scattering setup. Briefly, a collimated argon ion laser beam with $\lambda = 488 \text{ nm}$ is focused on a laponite sample. The scattered intensity, defined in arbitrary units for a normalized scattering volume, is detected at a given scattering angle $20^\circ \leq \theta \leq 120^\circ$, with a standard photomultiplier tube, and recorded using a parity conservation. As some of our samples are nonergodic, we must perform an ensemble-averaged measurement of the scattered intensity to obtain meaningful results [25,26]. This is done by slowly rotating the sample, while recording the scattered intensity. In this manner, the scattered intensity $I(q)$ for $0.2 \leq qd \leq 0.9$, where $q = (4\pi/\lambda)\sin(\theta/2)$ and $d = 30 \text{ nm}$ is the diameter of the laponite disks, is measured for both liquids and glassy solids.

Figure 3 shows the total scattered intensity defined by the limit of $I(q, \phi)$ for $q \rightarrow 0$ versus volume fraction ϕ for

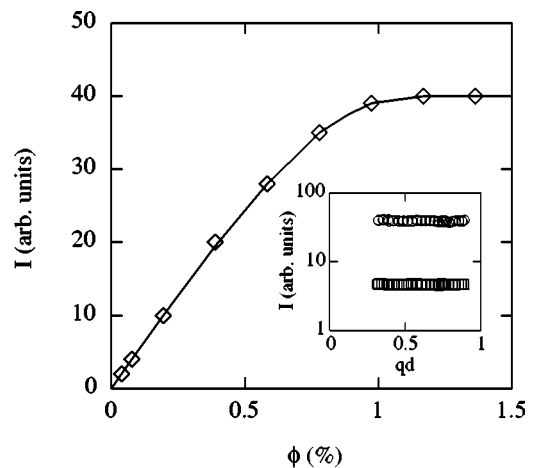


FIG. 3. Scattered intensity as a function of laponite volume fraction ϕ . The straight line is a guide for the eyes. The inset shows the variation of the scattered intensity for two laponite samples at different volume fractions, $\phi = 0.078\%$ (\square) and $\phi = 1.36\%$ (\circ).

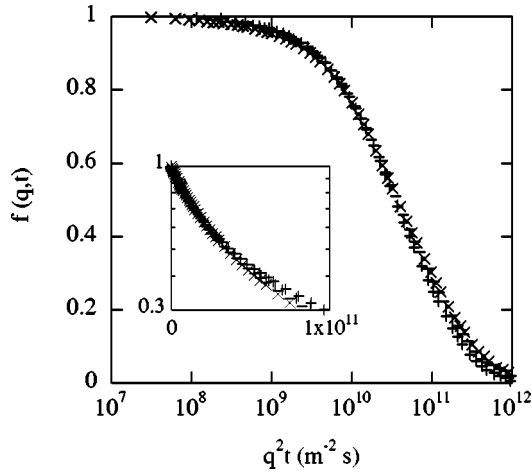


FIG. 4. Scaling of the dynamic structure factor of a laponite sample at $\phi=0.39\%$ measured at different scattering angles $\theta = 30^\circ$ (\times), $\theta=45^\circ$ ($-$), $\theta=60^\circ$ ($|$), $\theta=90^\circ$ ($+$). Inset: log-lin plot of the same data.

samples measured one week after sample preparation. For sufficiently large ϕ , the scattered intensity is weakly dependent on volume fraction. However, for volume fractions in the vicinity of ϕ^* , the scattered intensity begins to decrease with ϕ . Finally, for value of ϕ between 0.7% and 0.1%, the scattered intensity is proportional to the volume fraction of particles. Let us add that for very low volume fractions, a regime of strong electrostatic interactions can be observed, with slow modes, as in polyelectrolytes. We will not discuss this very dilute regime in this paper. The inset of Fig. 3 shows scattered intensity versus qd for a “liquid” laponite suspension ($\phi=0.078\%$, \square) and a “glassy solid” one ($\phi=1.36\%$, \circ).

As reported previously [22], for both volume fractions, the total intensity of scattered light $I(q)$ is independent of q over the whole range probed by solid laponite suspension (SLS). This q independence demonstrates that concentration fluctuations are random at any length scale probed by light scattering and indicates a disordered arrangement of laponite particles even in the glassy phase. We note also that for any given concentration, the total scattered intensity actually decreases with the age of the sample [22].

B. Fast relaxation

To investigate the collective dynamics of laponite suspensions, we have performed dynamic light scattering measurements on suspensions above and below the transition volume fraction ϕ^* as a function of wave number q and sample age t_w .

In Fig. 4, we have plotted the dynamic structure factor $f(q,t)$ versus $q^2 t$ for a dilute laponite solution ($\phi=0.39\%$) for several scattering angles: $\theta=30^\circ$ (\times), $\theta=45^\circ$ ($-$), $\theta=60^\circ$ ($|$), $\theta=90^\circ$ ($+$). These scattering angles span a range of wave numbers from $q=0.0089\text{ nm}^{-1}$ to $q=0.02422\text{ nm}^{-1}$. Notice that plotting $f(q,t)$ versus $q^2 t$ leads to a single master curve, indicating that the relaxation process is diffusive. The inset of Fig. 4 shows the data replotted on a log-lin scale. This representa-

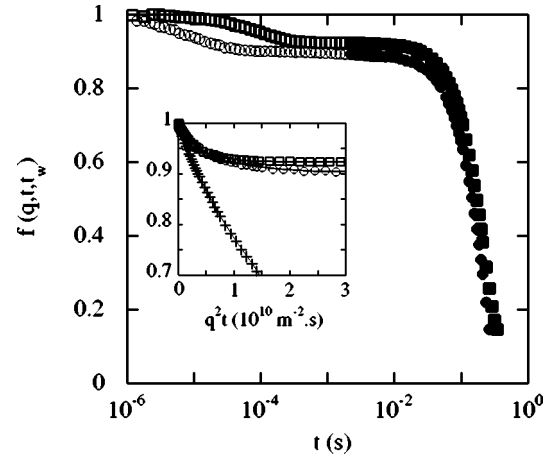


FIG. 5. Dynamic structure factor of a nonergodic sample ($\phi=1.36\%$) at scattering angles $\theta=90^\circ$ (\circ) and $\theta=20^\circ$ (\square). The decay shown by the filled symbols comes from sample rotation. Inset: scaling of the dynamic structure factor versus $q^2 t$. ($+$) are from a liquid sample $\phi=0.39\%$ at $\theta=90^\circ$.

tion shows that the process is not a simple exponential relaxation over the whole explored range, presumably reflecting the repulsive interactions between particles.

Above ϕ^* , the dynamical behavior of laponite suspensions is much more complex than below ϕ^* because of a two-stage relaxation process, and of the time dependence of the slow mode. However, the short time component of the dynamic structure factor can be measured by doing an ensemble-averaged measurement. Figure 5 shows the short time behavior of $f(q,t,t_w)$ at $\theta=20^\circ$ and 90° for a $\phi=1.36\%$ sample one week after preparation. For each scattering angle, there is a fast relaxation with a characteristic time close to τ_l (the characteristic time for liquid samples). Note that the amplitude of this fast relaxation process becomes smaller as the volume fraction ϕ increases. The artificial decorrelation of the dynamic structure factor, represented by the filled symbols at $t=2 \times 10^{-3}\text{ s}$ is due to the slow rotation of the sample. The inset of Fig. 5 shows $f(q,t,t_w)$ versus $q^2 t$. For comparison, the dynamic structure factor for a liquid sample [$\phi=0.39\%$, $\theta=90^\circ$ ($+$)] is also shown. Let us remark that the asymptotic dependences at very small $q^2 t$, which define the short relaxation time, are nearly indistinguishable. This is a signature of a diffusive process. More precisely, these results indicate that liquidlike ($\phi < \phi^*$) and glassy ($\phi > \phi^*$) laponite suspensions exhibit common short time dynamical behavior. Furthermore, the fast relaxation does not depend on the age of the sample, as illustrated in Fig. 6 for a 1.36% volume fraction sample.

The inset of Fig. 6 shows the effective diffusion coefficient versus laponite volume fraction. D_l is obtained from the measure of the relaxation time τ_l of the concentration fluctuations, defined by the asymptotic dependence of the dynamic structure factor at short time. Analysis of Fig. 6 shows that the relaxation time of the concentration fluctuations does not depend on the state (liquid or glassy solid) or the age of the laponite suspension and thus describes Brownian diffusion on a length scale dependent on the volume fraction of laponite particles.

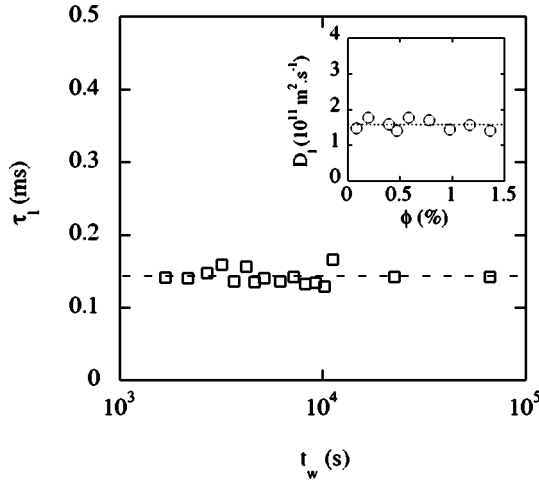


FIG. 6. Fast relaxation time τ_1 measured at $\theta=90^\circ$ versus aging time t_w for a glassy laponite suspension at $\phi=1.36\%$. Inset: diffusion coefficient D_1 of laponite samples versus volume fraction.

Let us finally make an observation about the q dependence of the intermediate plateau of the dynamic structure factor. We can try to understand this behavior within the framework of the “caged-particle” model developed by Pusey and Van Megen [25] as has been attempted for laponite in Ref. [20]. In this classical caged-particle picture of glassy dynamics, any given particle is described as being trapped in a transient cage formed by its surrounding neighbors. The motion of such a particle is described as a superposition of fast diffusive displacement of the particle within its cage and a slow activated process of escape from the cage. For a sufficiently large separation of the time scales, the analysis of the fast relaxation and the glassy plateau height may be simplified by regarding the slow relaxation as being frozen. One such simplified picture is the harmonically bound Brownian particle model [25,27]. In this model, the mean square displacement $\langle \Delta r^2(t) \rangle$ of a tracer particle is given by

$$\langle \Delta r^2(t) \rangle = \delta^2 \left[1 - \exp\left(-\frac{D_1 t}{\delta^2}\right) \right], \quad (3)$$

where δ is the characteristic cage size and where $D_1 \sim kT/6\pi\eta R$ is the effective diffusion coefficient of a particle of radius R in a medium with an effective viscosity η . Incoherent scattering from an ensemble of such caged particles leads to a strongly q -dependent plateau of $f(q,t)$ of the form

$$f_p(q) \sim \exp(-\delta^2 q^2). \quad (4)$$

Clearly, our results can not be described by such a classical “caged-particle” model, as we have found that $f_p(q)$ is only very weakly dependent on q . This is illustrated by Fig. 7 which presents a log-lin plot of $f_p(q)$ versus $q^2 d^2$. In fact, one would only expect cage-particle behavior for a system composed of dilute labeled particles, whereas our scattering measurements clearly probe collective fluctuations of the entire suspension of particles.

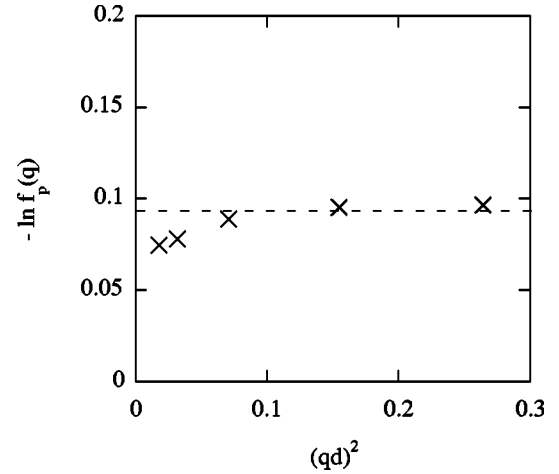


FIG. 7. Plot of the intermediate plateau of the dynamic structure factor $f_p(q)$ versus $q^2 d^2$, for a 1.36% volume fraction sample. The q dependence is incompatible with a cage-particle model.

C. Slow relaxations

Using the multispeckle technique, we have explored the behavior of the slow relaxation process. The ensemble-averaged intensity correlation functions is measured at different aging times t_w , after a quench into the glassy phase, for a $\phi=1.36\%$ volume fraction solution. $g^{(2)}(q,t,t_w)-1$ decays to zero on time scales that vary as a function of t_w from a few seconds to thousands of seconds. These measurements clearly underline the non-stationary nature of the relaxation of concentration fluctuations at long correlation times. This relaxation process reflects the aging dynamics in the glassy state. The corresponding dynamic structure factor $f(q,t,t_w)$ is presented in Fig. 8. The relaxation process can be described in terms of a power law $t^{-\alpha}$ —corresponding to the crossover from short to long time dynamics—multiplied by a stretched exponential relaxation. More precisely, we fit the data with

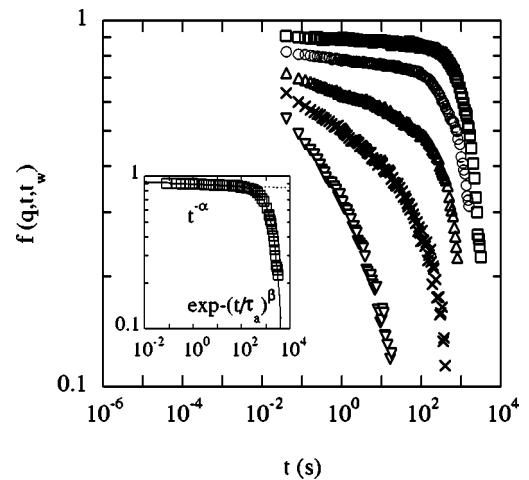


FIG. 8. Dynamic structure factor of a 1.36% laponite suspension ($q=0.03306 \text{ nm}^{-1}$, $\theta=150^\circ$) at different aging time: $t_w=8940 \text{ s}$ (∇), 10620 s (\times), 13800 s (Δ), 20040 s (\circ), 53040 s (\square). Inset: dynamic structure factor at $t_w=53040 \text{ s}$ and the corresponding fit to $at^{-\alpha}\exp[-(t/\tau_a)^\beta]$ with $a=0.88$, $\alpha=0.0055$, $\tau_a=2700 \text{ s}$, $\beta=1.35$.

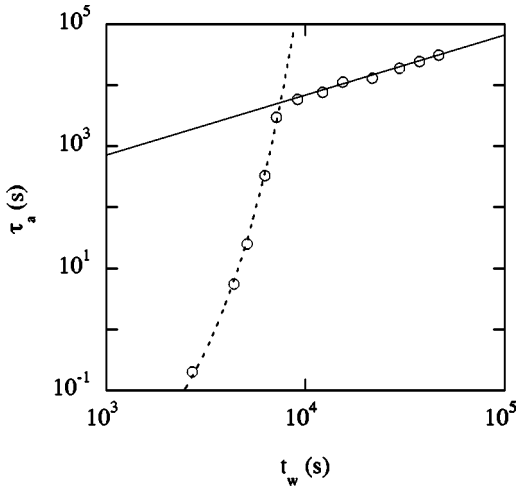


FIG. 9. Evidence of two distinct aging regimes: exponential aging and full aging. Data are obtained on a 1.36% laponite volume fraction sample at $\theta=30^\circ$.

$$f(q, t, t_w) = at^{-\alpha} \exp[-(t/\tau_a)^\beta] \quad (5)$$

(see inset of Fig. 8), where τ_a is a terminal relaxation time, and a is the amplitude of the process. This expression is familiar from the description of relaxation processes in generic glassy systems. Actually a , τ_a , α and β are all t_w -dependent.

Let us first discuss the aging dependence of the terminal relaxation time. Figure 9 shows τ_a as a function of t_w . Two distinct regimes of aging are evident. At short aging times, τ_a strongly increases with t_w . The dashed line in Fig. 9 is an exponential fit to the data for this regime of the form

$$\tau_a \sim \exp(bt_w). \quad (6)$$

In contrast, for long aging times τ_a has a power-law dependence on t_w ,

$$\tau_a \sim t_w^y, \quad (7)$$

with $y = 1.0 \pm 0.1$. This corresponds in fact to full aging [9]. It is important to note that the above results are not sensitive to the fitting procedure. In the regime of full aging where a is a constant, the fit gives $\alpha \approx 0.001$ and $\beta = 1.35 \pm 0.15$. Since α is very small, the $t^{-\alpha}$ term plays no role in the fitting procedure, and any arbitrary criterion for the relaxation time [e.g., the time for the decay of $f(q, t, t_w)$ to reach any particular fraction of its plateau value] would yield the same $\tau_a(t_w)$ dependence, up to a prefactor. The determination of the parameters in the exponential regime is, however, more difficult. In this regime, α is large enough that the relaxation is dominated by the $t^{-\alpha}$ prefactor, and the determination of τ_a and β is quite sensitive to details. Nevertheless, the exponential dependence of τ_a on t_w remains robust in this regime.

Let us now address the q dependence of the relaxation time τ_a . Figure 10 shows the variation of τ_a versus t_w for two values of q . In the exponential regime, as the scaling of τ_a is fragile, we cannot make quantitative conclusions about

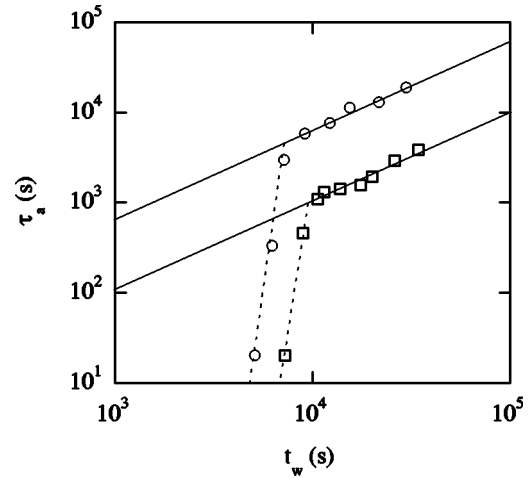


FIG. 10. Plot of τ_a versus t_w at two scattering angles $\theta=30^\circ$ (\circ) and $\theta=150^\circ$ (\square). The crossover from exponential to full-aging regime depends on q .

the q dependence of τ_a , or the crossover to the full-aging regime. However, definitive conclusions can be drawn about the behavior within the full-aging regime. The ratio of q^2 is 14 for the corresponding angles. However, the corresponding ratio of relaxation times in Fig. 10 is certainly less than a factor of 10. This rules out a simple q^2 dependence. We have measured, for a given sample, this q dependence in the regime of full aging, for four scattering angles. Figure 11 shows the prefactor τ_a/t_w as a function of $1/q$. As explained above, it is quite difficult to obtain a precise q dependence of this quantity. However, the data seems to follow a scaling law of the form

$$\tau_a(q, t_w) \sim q^{-x} t_w, \quad (8)$$

with $x = 1.3 \pm 0.1$. Moreover, in the full-aging regime, we observe that the behavior of the dynamic structure factor, in the q range explored, has the simple form

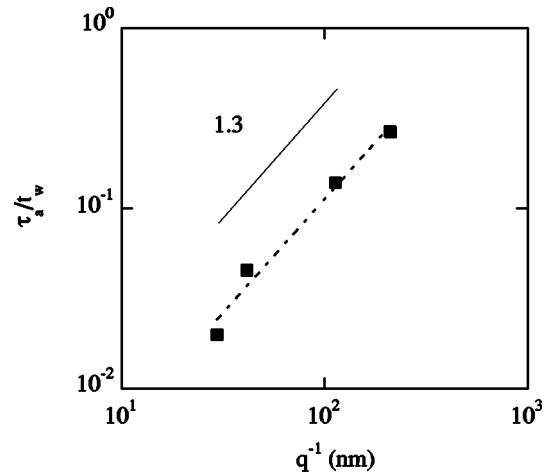


FIG. 11. q dependence of τ_a in the full-aging regime, for a 1.36% laponite volume fraction sample.

$$f(q, t, t_w) = \exp\left[-m\left(q^x \frac{t}{t_w}\right)^\beta\right], \quad (9)$$

where m is a constant depending on the volume fraction, and where $x \approx 1.3$ and $\beta \approx 1.35$.

IV. DISCUSSION

We have made comparative static and dynamic light scattering studies of laponite suspensions as a function of laponite volume fraction ϕ , wave number q , and sample age t_w . In making these measurements, special care was taken to properly account for the effects of nonequidispersity. We have utilized a combination of time-averaged measurements on slowly rotated samples (to probe relatively fast dynamics) and multispeckle ensemble-averaged measurements using a CCD camera (to probe slow dynamics). This combination of methods allowed us to obtain meaningful and accurate light scattering data from glassy laponite samples, and to fully explore the spatial and temporal dependence of their aging phenomena.

Laponite suspensions prepared at $\phi > \phi^*$ are initially liquidlike, and exhibit a single diffusive relaxation of the dynamic structure factor $f(q, t, t_w)$. With increasing age, such samples gradually thicken to form soft solids. $f(q, t, t_w)$ for these soft solids exhibits the classical two-stage relaxation behavior of glassy systems, consisting of a fast relaxation to a glassy plateau followed by a slow relaxation of this plateau that depends explicitly on the age of the sample (cf. Fig. 2). Although the fast and slow dynamics of these soft glassy solids are q dependent, the total intensity of scattered light, $I(q, \phi)$, is independent of q over the range of available wave vectors (cf. Fig. 3), indicating that these samples are spatially homogeneous and that relaxation dynamics are not due to any structural reorganization processes on these length scales.

The fast diffusive relaxation process is associated with unhindered diffusive motion of the laponite particles over concentration-dependent length scales. It is apparently a universal feature of the system, being present in both liquid and solid samples, and insensitive to volume fraction and sample age (cf. Figs. 5 and 6).

The slow relaxation process is more complex and exhibits two regimes as a function of sample age: an initial exponential aging regime, in which $\tau_a \sim \exp(t_w)$, separated by a relatively sharp crossover from a regime of full aging, in which $\tau_a \sim t_w$ (cf. Fig. 9). This key result provides a unified picture of aging for glassy laponite samples. Previous work using traditional time-averaged DLS techniques [20,21] have observed the exponential aging regime on short time scales, $\tau_a < 1$ s. Our multispeckle DLS technique allowed us to extend the range of time scales to access the full-aging regime at large τ_a and t_w in which the samples are nonergodic. We have previously observed this full-aging behavior in DWS studies of latex tracer particles in glassy laponite suspensions [22]. Such full-aging behavior has also been observed in measurements of response and correlation functions for a number of other soft glassy materials [28–30], and has been the subject of recent theoretical studies [9–11]. Moreover,

the two-stage aging behavior reported here has also been observed in networks of attractive colloidal particles [28], a very different system from homogenous glassy laponite suspensions. Let us add also the following comment. It is obviously impossible to detect a relaxation time larger than t_w . But the fact that $\tau_a \sim t_w$ is not an experimental artifact, but means that the system enters in an intrinsic transient regime of relaxation. Moreover, this is clearly revealed if one notices that τ_a depends on q . This q dependence of the aging regime will now be discussed.

The slow relaxation processes have significant q dependence. The fast and slow relaxation modes in the exponential aging regime are not well separated in time. As a result, the wave vector dependence of the exponential aging modes is difficult to quantify. However, the crossover age marking the end of this regime is clearly an increasing function of q , as shown in Fig. 10. In the full aging regime, the dynamic structure factor relaxes hyperdiffusively with a stretched exponential factor $\beta \approx 1.35$ and a q -dependent relaxation time that scales as $\tau_a \sim q^{-x}$ with $x \approx 1.3$, as indicated in Eqs. (8) and (9). One may try to connect the exponents x and β using the following spatial homogeneity hypothesis. In general, the dynamic structure factor may be expressed in the form $f(q, t) \sim \exp[-q^2 \langle \Delta r^2(t) \rangle]$, where $\langle \Delta r^2(t) \rangle$ is related to the mobility of individual scattering objects. Together with Eqs. (8) and (9), this implies a constraining relation between these exponents: $x\beta = 2$. Our data indicates $x\beta = 1.8 \pm 0.2$, which is compatible with this result.

The hyperdiffusive relaxation observed at long times is consistent with our previous DWS results on laponite suspensions [22], even if in this previous work we have noticed that the introduction of latex particles slightly decreases the pH of the solution (~ -0.5). Moreover, this behavior has also been reported in other (very different) systems [28,29]. A convincing generic mechanism for such hyperdiffusive relaxation has not yet been developed. However, it is probable that this behavior is associated with the relaxation of residual stress in metastable glassy systems. In the case of laponite suspensions, the q independence of the static scattered intensity at any given age indicates that this stress relaxation is *not* associated with any observable structural evolution. Rather, the stress release in this case is likely due to very local, synergistic rearrangements—occurring on the particle scale—which affect the stress field on larger length scales, as also proposed in Refs. [28,29]. The unusual temporal scaling of the dynamic structure factor for $t_w \geq \tau_a$ may originate in the way the stress relaxes due to these localized events [31]. However, additional experimental and theoretical work is necessary to clarify these issues.

V. CONCLUSION

We have measured the dynamic structure factor of light scattered by salt-free laponite solutions. This system exhibits no structure in SLS measurements. However, DLS measurements indicate that a clear two-step relaxation process occurs. The fast relaxation process consists of free Brownian motion of particles over a distance depending on the volume

fraction. The slow relaxation time has first an exponential dependence on the age of the system, and finally exhibits a full-aging behavior with a terminal relaxation time that is proportional to the age of the sample. The dynamic structure factor during the terminal relaxation regime also exhibits hyperdiffusive behavior that is not yet well understood on a fundamental level.

ACKNOWLEDGMENTS

Financial support from the NSF and the CNRS through a NSF-CNRS U.S.–France Cooperative Research grant (Grant No. NSF INT-9910103), and from the ACS Petroleum Research Fund (Grant No. ACS-PRF 36411-AC9) is gratefully acknowledged.

-
- [1] H. Van Olphen, *An Introduction to Clay Colloid Chemistry*, 2nd ed. (Wiley, New York, 1977).
- [2] S.D. Lubetkin, S.R. Middleton, and R.H. Ottewill, *Philos. Trans. R. Soc. London, Ser. A* **311**, 353 (1984).
- [3] T.F. Tadros, *Adv. Colloid Interface Sci.* **46**, 1 (1993).
- [4] P.F. Luckham and S. Rossi, *Adv. Colloid Interface Sci.* **82**, 43 (1999).
- [5] S. Jogun and C.F. Zukoski, *J. Rheol.* **40**, 1211 (1996).
- [6] N. Willenbacher, *J. Colloid Interface Sci.* **182**, 501 (1996).
- [7] S. Cocard, J.F. Tassin, and T. Nicolai, *J. Rheol.* **44**, 585 (1999).
- [8] J.P. Bouchaud, L.F. Cugliandolo, and J. Mézard Kurchan, in *Spin Glasses and Random Fields*, edited by A.P. Young (World Scientific Press, Singapore, 1998).
- [9] J.P. Bouchaud, in *Soft and Fragile Matter: Nonequilibrium Dynamics, Metastability and Flow*, edited by M.E. Cates, Scottish University Summer School in Physics, Vol. 53 (Institute of Physics, London, 2000).
- [10] P. Sollich, F. Lequeux, P. Hebraud, and M.E. Cates, *Phys. Rev. Lett.* **78**, 2020 (1997).
- [11] S.M. Fielding, P. Sollich, and M.E. Cates, *J. Rheol.* **44**, 323 (2000).
- [12] A. Liu and S.R. Nagel, *Nature (London)* **396**, 21 (1998).
- [13] D.W. Thompson and J.T. Butterworth, *J. Colloid Interface Sci.* **151**, 236 (1992).
- [14] J.D.F. Ramsay, *J. Colloid Interface Sci.* **109**, 441 (1986); R.G. Avery and J.D.F. Ramsay, *ibid.* **109**, 448 (1986).
- [15] A. Mourchid, A. Deville, J. Lambard, E. Lecolier, and P. Levitz, *Langmuir* **11**, 1942 (1995); A. Mourchid, E. Van Lecolier, H. Damme, and P. Levitz, *ibid.* **14**, 4718 (1998).
- [16] A. Mourchid and P. Levitz, *Phys. Rev. E* **57**, 4887 (1998).
- [17] M. Kroon, G.H. Wegdam, and R. Sprik, *Phys. Rev. E* **54**, 6541 (1996).
- [18] D. Bonn, H. Kellay, H. Tanaka, G. Wegdam, and J. Meunier, *Langmuir* **15**, 7534 (1999).
- [19] T. Nicolai and S. Cocard, *J. Colloid Interface Sci.* **244**, 51 (2001).
- [20] D. Bonn, H. Tanaka, G. Wegdam, H. Kellay, and J. Meunier, *Europhys. Lett.* **45**, 52 (1998).
- [21] B. Abou, D. Bonn, and J. Meunier, *Phys. Rev. E* **64**, 021510 (2001).
- [22] A. Knaebel, M. Bellour, J.-P. Munch, V. Viasnoff, F. Lequeux, and J.L. Harden, *Europhys. Lett.* **52**, 73 (2000).
- [23] S. Kirsch, V. Frenz, W. Schartl, E. Bartsch, and H. Sillescu, *J. Chem. Phys.* **104**, 1758 (1996).
- [24] L. Cipelletti and D.A. Weitz, *Rev. Sci. Instrum.* **70**, 3214 (1999).
- [25] P.N. Pusey and W. Van Megen, *Physica A* **157**, 705 (1989).
- [26] G. Nisato, P. Hebraud, J.-P. Munch, and S.J. Candau, *Phys. Rev. E* **61**, 2879 (2000).
- [27] J.Z. Xue, D.J. Pine, S.T. Milner, X.-L. Wu, and P.M. Chaikin, *Phys. Rev. A* **46**, 6550 (1992).
- [28] L. Cipelletti, S. Manley, R.C. Ball, and D.A. Weitz, *Phys. Rev. Lett.* **84**, 2275 (2000).
- [29] L. Ramos and L. Cipelletti, *Phys. Rev. Lett.* **87**, 778 (2001).
- [30] M. Cloitre, R. Borrega, and L. Leibler, *Phys. Rev. Lett.* **85**, 4819 (2000).
- [31] J.-P. Bouchaud and E. Pitard, *Eur. Phys. J.* **6**, 231 (2001).